Angiotensin(1-7)-Stearic Acid Conjugate: Synthesis and Characterization

Tayfun ACAR[1]* iD **, Burcu UCAR[1]*** iD

[1]Yildiz Technical University, Faculty of Chemistry and Metallurgy Engineering, Department of Bioengineering, Istanbul, 34220, Turkey

Abstract: The novel coronavirus, SARS-CoV-2, broken out as the COVID-19 epidemic, is transported into the cytoplasm by angiotensin-converting enzyme-2 (ACE2), a key protein of the renin-angiotensin-system (RAS). ACE2 is a protective protein that reduces angiotensin (Ang) II, the bioactive component of RAS, by converting it to its potent antagonist, Ang-(1-7) peptide, in order to provide a pathophysiological response to stimuli. Although ACE-2 is upregulated especially in pulmonary endothelial cells and alveolar epithelial cells, downregulation of ACE-2 in the lung owing to loss of key regulatory factors explains the enzyme-dependent lethality of SARS-CoV-2. The N-terminal domain (NTD) of S1, one of the protein subunits of coronaviruses, is known to recognize acetylated sialic acids on glycosylated cell surface receptors. In this study, the stearic acid-peptide conjugate mimicking the sialic acid structure was synthesized, which will be able to balance uncontrolled inflammatory response and excessive cytokine production, and depending on these to suppress pneumonia and acute respiratory distress syndrome (ARDS), against SARS-CoV-2. It was expected that fatty acid acylation would greatly enhance cellular internalization and cytosolic distribution of the peptide through the cell membrane. Thus, we synthesized fatty acyl derivative of the N-Ac-Gly$_4$-Ang (1-7) peptide. The peptide was synthesized using Fmoc/tBu solid-phase peptide chemistry and characterized by FT-IR, Zetasizer, and LC-ESI-MS. This study provided more detailed insights into understanding and meeting the basic structural requirements for optimal cellular delivery and formulation of the stearyl Ang (1-7)-peptide conjugate.

INTRODUCTION

Coronaviruses (CoVs), classified within the family *Coronaviridae*, subfamily *Orthocoronavirinae*, are positive-sense single-stranded, enveloped viruses that are found in birds and mammals, prone to crossover between host species. Four different genera have been identified: Alpha, Beta, Gamma, and Delta coronavirus. CoVs, which can cause disease by transmitting from animals to humans, pose a constant threat to public health. Deadly respiratory coronaviruses have emerged three times in this century. While one of them, SARS, emerged towards the end of 2002 and disappeared by 2004,

the second one, MERS, emerged in 2012. Lastly, COVID-19, which broke out on 31 December 2019 and still continues, was characterized as an epidemic (pandemic) by WHO on 11 March 2020 (1-3).

As comprehensive genetic researches covering COVID-19, the virus is phylogenetically related to SARS-like bat viruses. For this reason, bats can be estimated as a potential principal reservoir. Although the intermediate source and source of transfer to humans is unknown, person-to-person rapid virus transmission has been approved. The transmission occurs mainly through direct contact or

through droplets emitted from an infected person as a result of coughing or sneezing (4, 5).

CoVs have positive polarity, single-stranded enveloped RNA viruses (6). The key viral proteins are membrane glycoprotein (M), nucleocapsid protein (N), and spike glycoprotein (S). SARS-CoV-2 diverges from past CoVs by encoding an additional glycoprotein with acetyl esterase and hemagglutination (HE) features (7). Most of the drug and vaccine investigation studies against COVID-19 seem to target spike protein. The spike protein comprises two subunits, S1 and S2, which are responsible for the replication of the virus. The RBD (receptor binding domain) of the S1 subunit interacts with ACE2 followed by the S2 subunit mediating the fusion between virus and host cell membranes, allowing viral RNA to be transported into the cytoplasm (6). CoVs typically have two domains within S1 that can bind to host receptors, an amino (N)-terminal domain (NTD) and a carboxy (C)-terminal domain (CTD) (8, 9). Acetylated sialic acids on glycosylated cell surface receptors are recognized by S1 NTD (10). A docking study showed that resembling sialic acid, peptides mimicking the sialic acid structure are recognized by the receptor-binding site in Hemagglutinin (11). Therefore, it is important to modify the molecules to be developed with sialic acid or to combine them with structures that can mimic sialic acid.

The novel coronavirus that caused the COVID-19 epidemic enters human cells by binding to ACE2 like the SARS coronavirus (12). ACE2 is a protective protein of the RAS that converts angiotensin (Ang) II, the biologically active basic peptide of the RAS, to its physiological antagonist, Ang-(1-7). The binding of SARS-CoV-2 to the ACE2 catalytic site decreases ACE2 expression, resulting in an increase in Ang II (12). Although ACE-2 is upregulated especially in pulmonary endothelial cells and alveolar epithelial cells, downregulation of ACE-2 in the lung due to loss of key regulatory factors explains the enzyme-dependent lethality of SARS-CoV-2 (13, 14).

Ang-(1-7) inhibits alveolar type II cell apoptosis against the damage caused by the virus in its progression to the brain, and reduces the activation of endothelial cells lining blood vessels. Thus, it reduces the loss of blood-brain barrier function and edema. Ang-(1-7) plays a crucial role in protecting against the development of pulmonary inflammation and idiopathic pulmonary fibrosis (IPF) in the course of very severe recurrent illness. Pneumonia and ARDS in the illness are accompanied by an uncontrolled inflammatory response and excessive cytokine production due to immune response dysregulation caused by the virus. This heptapeptide balances the uncontrolled release and synthesis of proinflammatory and profibrotic cytokines due to epithelial damage (13).

In this study, it was suggested that the increase of Ang-(1-7) concentration during viral infection may be vital for protection from endothelial cellular activation and pulmonary damage. Among other strategies, the use of Ang-(1-7) or one of its mimetics was considered a promising step to prevent damage and reduce the severity of COVID-19 infection in high-risk patients.

Bioconjugation is a chemical method used to bring two molecules, at least one of which is a biomolecule (peptide, protein, etc.), together with a covalent bond. Bioconjugation is a tool at the interface between chemistry and biology. Bioconjugation reactions are critical in the modification of peptides. Due to recent advances in the study of biomolecules, peptides can be designed to perform a variety of functions such as cellular monitoring, imaging, and target drug delivery (15-20).

Because of the reasons mentioned above, Ang-(1-7) peptide was studied and the peptide was modified. During peptide synthesis, the N-terminal end of the sequence was acetylated to form a sialic acid-like structure. The sialic acid mimic peptide was obtained by binding the peptide with stearic acid from the side chain. In this way, it is aimed to see a dual effect for the fight against the virus. In a study similar to this hypothesis, stearic acid-peptide conjugates (N-Stearoyl Peptides) that can mimic sialic acid have been developed for influenza virus-caused disease. (11, 21, 22). In summary, we designed and synthesized a novel Ang-(1-7) peptidomimetic against COVID-19 via N-terminal acetylation modification, and conjugation with stearic acid.

MATERIAL AND METHODS

All L-amino acids, HCTU (o-(1H-6-chlorobenzotriazole-1-yl)-1,1,3,3-tetramethyluronium hexafluorophosphate), HOBt.H_2O (1-hydroxybenzotriazole hydrate), Wang resin LL, EDC (1-ethyl-3-(3-dimethylaminopropyl)carbodiimide hydrochloride), stearic acid as well as organic solvents such as DMF, DCM, ACN, etc. were commercially available from Sigma Aldrich (St. Louis) in the USA. Ultra-pure water was supplied from a Millipore Milli-Q system. Molecules were drawn using *ChemDraw Ultra 12.0.*

The FT-IR spectra were obtained from Thermo Scientific Nicolet iS10 in ATR mode. Analyses were performed at room temperature in the wavenumber range of 4,000-650 cm^{-1} with a resolution of 4 cm^{-1}, and out of 32 scans. The background spectrum was obtained at ambient atmosphere before sample analysis (23).

The absorption spectra of each sample were monitored with a Shimadzu-2600 UV spectrophotometer within the wavelength range of 190-800 nm at 25 ± 1 °C (23).

LC-MS system with electrospray ionization (ESI) probe was used as the chromatographic system. 75 μL sample was injected into Shim-Pack MRC-ODS-C18 LC column (25 cm X 6 mm). The wavelength of the PDA detector was set to 210 and 280 nm. RP-HPLC analysis was carried out at room temperature. A gradient was applied from eluent A (dH$_2$O, 0.1% (v/v) FA) to eluent B (ACN, 0.1% (v/v) FA). The flow rate of the eluent was 0.6 mL/min. The ESI was operated in positive ion mode in the 200-1500 m/z range. The capillary temperature was kept at 250 °C. The flow rate of the nebulizer gas (N$_2$) was set at 1.5 L/min (24, 25).

The mean size and zeta potential of the samples were determined by Zetasizer Nano ZS (Malvern). Samples were dissolved in PBS (pH 7.2). Samples were diluted to 1:2 for the analysis and injected into a disposable capillary cell DTS1070 (Malvern Instruments, MA) and loaded onto the analyzer. Measurements were performed at 25 °C ± 1 °C with a material refraction index of 1.33, and viscosity of 0.8872 cp. All measurements were performed in triplicate (26).

Peptide Synthesis and Characterization
Angiotensin (1-7) peptide with four glycine amino acids added to its N-terminal was synthesized by Fmoc/*t*Bu solid-phase peptide chemistry. In addition, the N-terminal end of the sequence was modified by acetylation. The peptide sequence was as follows: N-Ac-GGGGDRVYIHP-COOH. First of all, the C-terminal of the peptide sequence was loaded onto unloaded Wang resin used as the solid phase. For this, 1 g of Wang resin LL (0.67 mmol/g) was swollen in 25 mL of DMF:DCM (1:9; v:v) for 30 minutes. According to the resin, 2 eq of Fmoc-Pro-OH and 2 eq of HOBt.H$_2$O were dissolved in a minimum amount of DMF and added to the resin mixture. According to the resin, 0.1 eq of DMAP (4-(Dimethylamino)pyridine) was dissolved in a minimum volume of DMF and added to the resin mixture simultaneously with 1 eq of DIC (N,N'-Diisopropylcarbodiimide) relative to the Fmoc-Pro-OH. Then, it was shaken at room temperature for six hours. The resin beads were washed three times with DMF, MeOH, DCM, and Et$_2$O, respectively. After the reaction, 2 eq of acetic anhydride and 2 eq of pyridine were added to the resin mixture according to the resin and shaken for 30 minutes to close the hydroxyl groups that remain unreacted on the resin beads. The resin beads were washed with DMF, MeOH, DCM, and Et$_2$O, respectively, three times, and dried under vacuum (27-29). The loading efficiency of the Wang resin was performed according to the literature based on the removal of Fmoc groups and UV-Vis analysis of Fmoc with using Equation 1 (30).

$$L = \frac{A \cdot v}{\varepsilon \cdot l \cdot m} \qquad \text{(Eq. 1)}$$

L: amino acid loading (mmol/g)
A: absorbance value at the 301 nm
v: dilution factor of solvent
ε: molar absorptivity of the Fmoc group at 301 nm (7800 L x mol^{-1} x cm^{-1})
l: light path length of the cell (1 cm)
m: weight of the loaded resin (mg)

For the synthesis of the peptide, 150 mg of the Fmoc-Pro-Wang resin was swollen in 25 mL of dry DMF: DCM (1:3, v/v) for 3 hours. After filter drying, a freshly prepared deprotection solution (20% piperidine in DMF) was added for removing Fmoc protecting groups. Washing was performed with an excess amount of DMF and DCM. The next amino acid solution, activator (HBTU (o-(Benzotriazol-1-yl)-N,N,N',N'-tetramethyluronium hexafluorophosphate), HOBt.H$_2$O), and activator base (NMP (N-methylpyrrolidone), DIEA (N,N-diisopropylethylamine)) solutions were added, respectively, and incubated for 1 hour. Then the above-mentioned washing process was done again. These processes (deprotection, activation, and coupling) were continued until all amino acids were added (26). The N-terminal end of the peptide was acetylated by adding 0.5M acetic anhydride solution together with 0.125 M DIEA and 0.015 M HOBt.H$_2$O in DMF. The resin was washed with MeOH, DCM and Et$_2$O, three times and dried under vacuum (19). The peptide was cleavaged from the resin with a cleavage cocktail (trifluoroacetic acid (TFA, 94% v/v):1,2-ethanedithiol (EDT, 2.5% v/v):triisopropylsilane (TIS, 1% v/v):dH$_2$O (2.5%, v/v)). The solution including the desired peptide was concentrated, the peptide was precipitated with cold Et$_2$O and separated by centrifugation. It was dissolved in 1:1 H$_2$O:ACN at a concentration of 1 mg/mL and characterized by LC-ESI-MS (19).

Conjugation of the Peptide with Stearic Acid
The stearic acid molecule was conjugated with the synthesized and characterized peptide sequence from the amine group at the side chain of the Arginine residue of the peptide sequence in the presence of EDC. For this, 0.1 mmol stearic acid (SA) solution in 10 mL of EtOH was prepared. For the activation, relative to SA 10 equivalents of EDC in pure water was added. Stearic acid peptide conjugation was performed by adding 1 equivalent of the peptide in sodium acetate buffer (pH 4.5) after 1 hour of activation. The mixture was stirred intensively overnight at 25 °C under nitrogen gas. The organic solvent was evaporated under vacuum followed by lyophilization. The resulting product was further washed with EtOH to remove the unreacted SA. Finally, the peptide-SA conjugate was redispersed in dH$_2$O and lyophilized. The molecular

weight of the lyophilized conjugate was determined by LC-ESI-MS (31, 32).

RESULTS AND DISCUSSION

Scheme 1 demonstrated the synthesis of the designed peptide and the conjugation reaction with stearic acid of the synthesized peptide. The coupling of amino acids to the resin, N-terminal modification of peptidyl resin with acetylation, cleavage of the peptide, and conjugation of stearic acid to the peptide, and other respectively applied methods were shown schematically.

For the solid phase peptide synthesis, unloaded Wang resin was loaded with Fmoc-Pro-OH. The resin substitution was determined by the Fmoc removal process. This process was based on the spectroscopic determination of the Fmoc and its dibenzofulvene-piperidine derivatives after deprotection of the resin with a deprotection solution. 1 mL of freshly prepared 20% piperidine solution in DMF was added onto a certain amount of

the Fmoc-Pro-Wang resin in an Eppendorf tube. After 15 minutes of shaking in an incubator, a minute was kept on hold for the precipitation of resin beads. UV-Vis spectrum of the supernatant phase (diluted by 10 times with DMF) was recorded. The resin substitution of Fmoc-Pro-Wang was found as 0.33 mmol/g (Figure 1). The resin substitution for commercially available Fmoc-Pro-Wang resin produced by different companies ranges between 0.2-0.8 mmol/g (33, 34).

ESI-MS is often preferred both in determining the average molecular weight of degradation products of biomolecules such as proteins and enzymes and in verifying the molecular weights of materials with smaller molecular weights such as peptides (35, 36). In this study, we applied the ESI-MS method to verify the molecular weight of the peptide. The obtained spectrum of the peptide was given in Figure 2 and the mass of the peptide was calculated as follows:

$[M + 3Na]^{3+} = 412.5$ Da $\Rightarrow M_{exp} = 1168.5$ Da $M_{calc} = 1169.25$ Da

Scheme 1: Illustration of synthesis mechanism of the stearyl peptide conjugate.
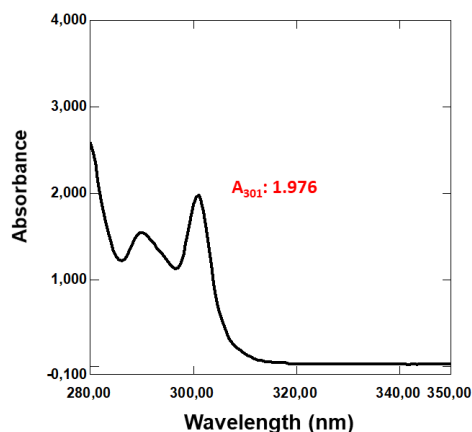
Figure 1: UV-Vis spectrum of dibenzofulvene-piperidine by-product formed after the removal of the Fmoc group (A_{301}: 1.976).
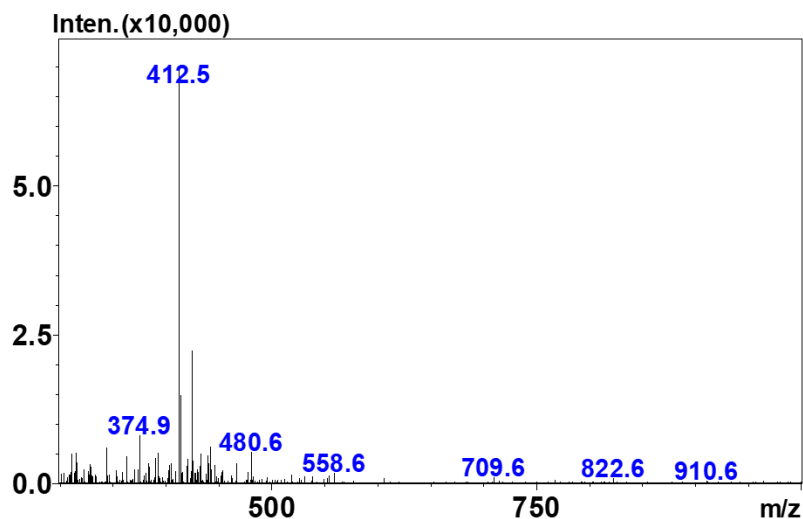
Figure 2: ESI-MS spectrum of the N-Ac-Gly$_4$-Ang (1-7) peptide.
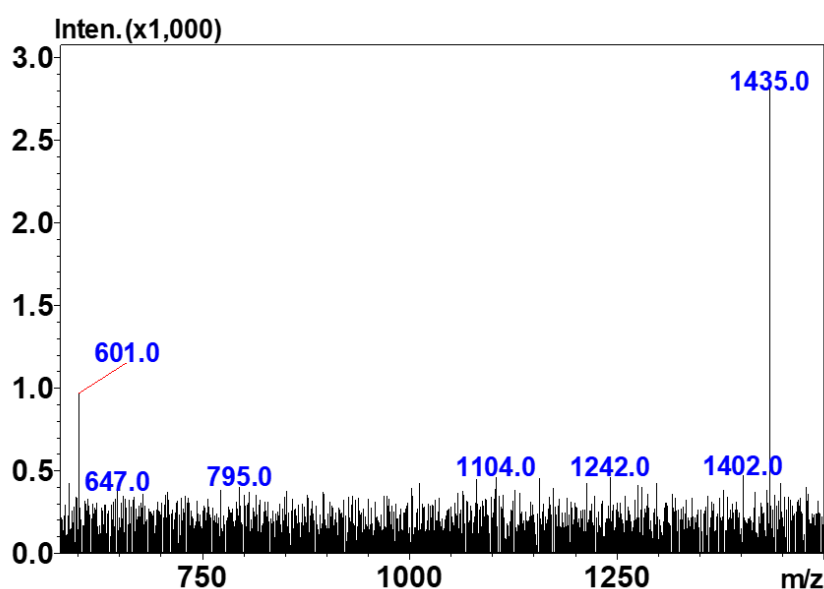
Figure 3: ESI-MS spectrum of the peptide-stearic acid conjugate.

The stearyl peptide conjugate of stearic acid and N-Ac-Gly$_4$-Ang (1-7) was synthesized by carbodiimide chemistry. Unreacted EDC and its o-acylisourea byproduct and unreacted stearic acid were removed from the environment with post-synthesis washing processes. The conjugate was characterized by LC-ESI-MS. As illustrated in Figure 3, ESI-MS ion peak at 1435.0 confirmed the formation of the conjugate. [M] = 1435.0 Da $\Rightarrow$ M$_{exp}$ = 1435.0 Da   M$_{calc}$ = 1435.73 Da

FT-IR analysis was performed to evaluate the changes of functional groups in peptide and stearic acid after conjugation reaction. The conjugation reaction was carried out between the -COOH groups of stearic acid and the amine group of the arginine residue of the peptide. Therefore, it is expected that there will be a change in the peaks of these groups.

FT-IR spectrum of the stearyl peptide conjugate was comparatively given with stearic acid and peptide in Figure 4. Some of the basic peaks of the peptide were N-H stretching at 3276.5 cm^{-1}, -CH$_2$ stretching at 2976.6 cm^{-1}, C=O (carboxylic acid) stretching 1734.7 cm^{-1}, C=O (amide I) stretching 1680.7 and 1628.6 cm^{-1}, and amide II band resulting from N-H bending and C-N stretching at 1548.1 cm^{-1}. It can be understood from the FT-IR spectrum of stearic acid that the band at 1629.6 cm^{-1} was C=O stretching of carboxyl and the broad peaks at 2915.8 and 2848.8 cm^{-1} were C-H stretching. The peak around 719.7 cm^{-1} corresponded to the bending vibration of long (CH$_2$)$_n$ chains of stearic acid. In the stearyl peptide spectrum, the presence of N-H stretching of the peptide at 3275.0 cm^{-1}, the presence of C-H bendings around 2900 cm^{-1} of the stearic acid, and also the shifting of the carbonyl

peaks of the carboxylic acid and amide (seen at 1720.7 and 1641.1 cm^{-1}) supported the conjugation.
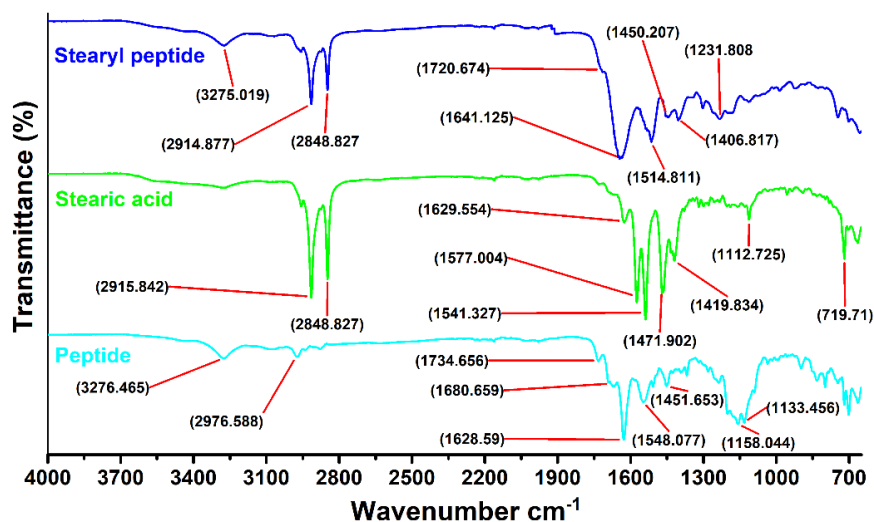
Figure 4: FT-IR spectrum of the stearyl peptide conjugate comparatively given with stearic acid and peptide.

Another methods we use to characterize the stearyl peptide conjugate were dynamic and electrophoretic light scattering measurements. The average size results obtained by the DLS method were given in Figure 5. The mean size of the peptide and stearic acid were 6.33 ± 0.996 and 8.55 ± 2.400 nm, respectively. The size of the obtained conjugate was measured as 25.92 ± 3.295 nm. With the combination of peptide and stearic acid after the conjugation reaction, the obtained structure got a little bigger and the average particle size increased (19).

Zeta potential values obtained from electrophoretic light scattering measurements for the peptide, stearic acid, and stearyl peptide conjugate were -6.20 ± 0.621, -17.20 ± 1.96, and -15.90 ± 1.53 mV, respectively (Figure 6). The zeta potential became more negative as a result of participating the amine groups of the peptide to the conjugation reaction and the C-terminal -COOH groups making the environment negatively charged (shift from -6.20 to -15.90 mV). With the addition of stearic acid -COOH groups to the reaction, the zeta potential value shifted slightly to positive (shift from -17.20 to -15.90 mV) (19).
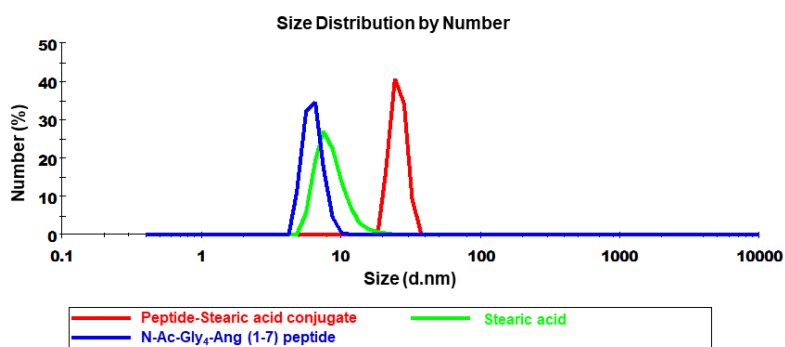
Figure 5: The particle size distribution of peptide, stearic acid, and stearyl peptide conjugate by number.
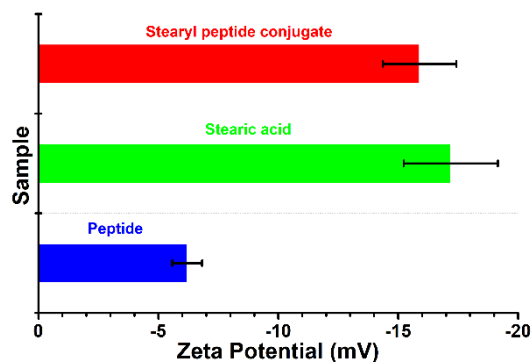
Figure 6: Zeta potential values of the peptide, stearic acid, and stearyl peptide conjugate.

CONCLUSION

Herein, modified angiotensin (1-7) peptide was synthesized by being N-terminal acetylation and four glycine adding. The molecular weight of the peptide was confirmed by LC-ESI-MS. The stearyl peptide conjugate of the N-Ac-Gly$_4$-Ang (1-7) with stearic acid was formed with carbodiimide chemistry using EDC. The characterization of the conjugate was performed by FT-IR, Zetasizer, and LC-ESI-MS methods. Changes in size, zeta potential values, FT-IR peaks of functional groups after conjugation and also mass analysis result supported the formation of the stearyl peptide conjugate. As future research, it is aimed to reveal more detailed information about the obtained conjugate by cellular studies.

REFERENCES

1. Xu Z, Shi L, Wang Y, Zhang J, Huang L, Zhang C, et al. Pathological findings of COVID-19 associated with acute respiratory distress syndrome. The Lancet Respiratory Medicine. 2020 Apr;8(4):420–2. <DOI>.

2. Duan K, Liu B, Li C, Zhang H, Yu T, Qu J, et al. Effectiveness of convalescent plasma therapy in severe COVID-19 patients. Proc Natl Acad Sci USA. 2020 Apr 28;117(17):9490–6. <DOI>.

3. Chen H, Guo J, Wang C, Luo F, Yu X, Zhang W, et al. Clinical characteristics and intrauterine vertical transmission potential of COVID-19 infection in nine pregnant women: a retrospective review of medical records. The Lancet. 2020 Mar;395(10226):809–15. <DOI>.

4. Rothan HA, Byrareddy SN. The epidemiology and pathogenesis of coronavirus disease (COVID-19) outbreak. Journal of Autoimmunity. 2020 May;109:102433. <DOI>.

5. Shereen MA, Khan S, Kazmi A, Bashir N, Siddique R. COVID-19 infection: Emergence, transmission, and characteristics of human coronaviruses. Journal of Advanced Research. 2020 Jul;24:91–8. <DOI>.

6. Dhama K, Sharun K, Tiwari R, Dadar M, Malik YS, Singh KP, et al. COVID-19, an emerging coronavirus infection: advances and prospects in designing and developing vaccines, immunotherapeutics, and therapeutics. Human Vaccines & Immunotherapeutics. 2020 Jun 2;16(6):1232–8. <DOI>.

7. Kannan S, Shaik Syed Ali P, Sheeza A, Hemalatha K. COVID-19 (Novel Coronavirus 2019) – recent trends. European Review for Medical and Pharmacological Sciences. 2020 Feb;24(4):2006–11. <DOI>.

8. Hurdiss DL, Drulyte I, Lang Y, Shamorkina TM, Pronker MF, van Kuppeveld FJM, et al. Cryo-EM structure of coronavirus-HKU1 haemagglutinin esterase reveals architectural changes arising from prolonged circulation in humans. Nat Commun. 2020 Dec;11(1):4646. <DOI>.

9. Bakkers MJG, Lang Y, Feitsma LJ, Hulswit RJG, de Poot SAH, van Vliet ALW, et al. Betacoronavirus Adaptation to Humans Involved Progressive Loss of Hemagglutinin-Esterase Lectin Activity. Cell Host & Microbe. 2017 Mar;21(3):356–66. <DOI>.

10. Kirchdoerfer RN, Cottrell CA, Wang N, Pallesen J, Yassine HM, Turner HL, et al. Pre-fusion structure of a human coronavirus spike protein. Nature. 2016 Mar;531(7592):118–21. <DOI>.

11. Matsubara T, Onishi A, Saito T, Shimada A, Inoue H, Taki T, et al. Sialic Acid-Mimic Peptides As Hemagglutinin Inhibitors for Anti-Influenza Therapy. J Med Chem. 2010 Jun 10;53(11):4441–9. <DOI>.

12. Zhang H, Penninger JM, Li Y, Zhong N, Slutsky AS. Angiotensin-converting enzyme 2 (ACE2) as a SARS-CoV-2 receptor: molecular mechanisms and potential therapeutic target. Intensive Care Med. 2020 Apr;46(4):586–90. <DOI>.

13. Santos RAS, Sampaio WO, Alzamora AC, Motta-Santos D, Alenina N, Bader M, et al. The ACE2/Angiotensin-(1–7)/MAS Axis of the Renin-Angiotensin System: Focus on Angiotensin-(1–7). Physiological Reviews. 2018 Jan 1;98(1):505–53. <DOI>.

14. Kuba K, Imai Y, Rao S, Gao H, Guo F, Guan B, et al. A crucial role of angiotensin converting enzyme 2 (ACE2) in SARS coronavirus–induced lung injury. Nat Med. 2005 Aug;11(8):875–9. <DOI>.

15. Amin HH, Meghani NM, Oh KT, Choi H, Lee B-J. A conjugation of stearic acid to apotransferrin, fattigation-platform, as a core to form self-assembled nanoparticles: Encapsulation of a hydrophobic paclitaxel and receptor-driven cancer targeting. Journal of Drug Delivery Science and Technology. 2017 Oct;41:222–30. <DOI>.

16. Khan AA, Alanazi AM, Jabeen M, Chauhan A, Abdelhameed AS. Design, synthesis and in vitro anticancer eval-

uation of a stearic acid-based ester conjugate. Anticancer research. 2013;33(6):2517–24.

17. Wang Y, Cheetham AG, Angacian G, Su H, Xie L, Cui H. Peptide–drug conjugates as effective prodrug strategies for targeted delivery. Advanced Drug Delivery Reviews. 2017 Feb;110–111:112–26. <DOI>.

18. Hoppenz P, Els-Heindl S, Beck-Sickinger AG. Peptide-Drug Conjugates and Their Targets in Advanced Cancer Therapies. Front Chem. 2020 Jul 7;8:571. <DOI>.

19. Ucar B, Acar T, Pelit-Arayici P, Demirkol MO, Mustafaeva Z. A new radio-theranostic agent candidate: Synthesis and analysis of (ADH-1) c-EDTA conjugate. Fresenius Environmental Bulletin. 2018;27(7):4751–8.

20. Ucar B, Acar T, Arayici PP, Sen M, Derman S, Mustafaeva Z. Synthesis and applications of synthetic peptides. In: Peptide Synthesis. IntechOpen; 2019.

21. Heerze LD, Smith RH, Wang N, Armstrong GD. Utilization of sialic acid-binding synthetic peptide sequences derived from pertussis toxin as novel anti-inflammatory agents. Glycobiology. 1995;5(4):427–33. <DOI>.

22. Matsubara T. Potential of Peptides as Inhibitors and Mimotopes: Selection of Carbohydrate-Mimetic Peptides from Phage Display Libraries. Journal of Nucleic Acids. 2012;2012:1–15. <DOI>.

23. Cebeci C, Ucar B, Acar T, Erden I. Colorimetric detection of hydrogen peroxide with gadolinium complex of phenylboronic acid functionalized 4,5-diazafluorene. Inorganica Chimica Acta. 2021 Jul;522:120386. <DOI>.

24. Acar T, Pelit Arayıcı P, Ucar B, Karahan M, Mustafaeva Z. Synthesis, Characterization and Lipophilicity Study of Brucella abortus' Immunogenic Peptide Sequence That Can Be Used in the Future Vaccination Studies. Int J Pept Res Ther. 2019 Sep;25(3):911–8. <DOI>.

25. Ucar B. Synthesis and characterization of natural lanthanum labelled DOTA-Peptides for simulating radioactive Ac-225 labeling. Applied Radiation and Isotopes. 2019 Nov;153:108816. <DOI>.

26. Ucar B, Acar T, Arayici PP, Derman S. A nanotechnological approach in the current therapy of COVID-19: model drug oseltamivir-phosphate loaded PLGA nanoparticles targeted with spike protein binder peptide of SARS-CoV-2. Nanotechnology. 2021 Nov 26;32(48):485601. <DOI>.

27. Guillier F, Orain D, Bradley M. Linkers and Cleavage Strategies in Solid-Phase Organic Synthesis and Combinatorial Chemistry. Chem Rev. 2000 Jun 1;100(6):2091–158. <DOI>.

28. Chan W, White P, editors. Fmoc Solid Phase Peptide Synthesis: A Practical Approach [Internet]. Oxford University Press; 1999 [cited 2022 Feb 19]. <URL>.

29. Atherton E, Logan CJ, Sheppard RC. Peptide synthesis. Part 2. Procedures for solid-phase synthesis using N^{α}-fluorenylmethoxycarbonylamino-acids on polyamide supports. Synthesis of substance P and of acyl carrier protein 65–74 decapeptide. J Chem Soc, Perkin Trans 1. 1981;(0):538–46. <DOI>.

30. Al Musaimi O, Basso A, de la Torre BG, Albericio F. Calculating Resin Functionalization in Solid-Phase Peptide Synthesis Using a Standardized Method based on Fmoc Determination. ACS Comb Sci. 2019 Nov 11;21(11):717–21. <DOI>.

31. Hu F-Q, Zhang, Du Y-Z, Yuan. Brain-targeting study of stearic acid–grafted chitosan micelle drug-delivery system. IJN. 2012 Jun;3235. <DOI>.

32. Pereira P, Barreira M, Cruz C, Tomás J, Luís Â, Pedro AQ, et al. Brain-Targeted Delivery of Pre-miR-29b Using Lactoferrin-Stearic Acid-Modified-Chitosan/Polyethyleneimine Polyplexes. Pharmaceuticals. 2020 Oct 15;13(10):314. <DOI>.

33. Anonymous. AAPPTec. Resins for Solid Phase Peptide Synthesis [Internet]. AAPPTec. Resins for Solid Phase Peptide Synthesis. 2021 [cited 2022 Feb 19]. <URL>.

34. Anonymous. Sigma-Aldrich. Fmoc-Pro-Wang resin [Internet]. Sigma-Aldrich. Fmoc-Pro-Wang resin. 2021 [cited 2022 Feb 19]. <URL>.

35. Banerjee S, Mazumdar S. Electrospray Ionization Mass Spectrometry: A Technique to Access the Information beyond the Molecular Weight of the Analyte. International Journal of Analytical Chemistry. 2012;2012:1–40. <DOI>.

36. Zhang S (Weihua), Jian W. Recent advances in absolute quantification of peptides and proteins using LC-MS. Reviews in Analytical Chemistry [Internet]. 2014 Jan 1 [cited 2022 Feb 19];33(1). <DOI>.